Development 139, 4656-4665 (2012) doi:10.1242/dev.078923

The differentiation and movement of presomitic mesoderm progenitor cells are controlled by Mesogenin 1

Rita Fior[1,2,*], Adrienne A. Maxwell[3], Taylur P. Ma[4], Annalisa Vezzaro[5], Cecilia B. Moens[4], Sharon L. Amacher[3,‡], Julian Lewis[6] and Leonor Saúde[1,2,*]

SUMMARY

Somites are formed from the presomitic mesoderm (PSM) and give rise to the axial skeleton and skeletal muscles. The PSM is dynamic; somites are generated at the anterior end, while the posterior end is continually renewed with new cells entering from the tailbud progenitor region. Which genes control the conversion of tailbud progenitors into PSM and how is this process coordinated with cell movement? Using loss- and gain-of-function experiments and heat-shock transgenics we show in zebrafish that the transcription factor Mesogenin 1 (Msgn1), acting with Spadetail (Spt), has a central role. Msgn1 allows progression of the PSM differentiation program by switching off the progenitor maintenance genes *ntl*, *wnt3a*, *wnt8* and *fgf8* in the future PSM cells as they exit from the tailbud, and subsequently induces expression of PSM markers such as *tbx24*. *msgn1* is itself positively regulated by Ntl/Wnt/Fgf, creating a negative-feedback loop that might be crucial to regulate homeostasis of the progenitor population until somitogenesis ends. Msgn1 drives not only the changes in gene expression in the nascent PSM cells but also the movements by which they stream out of the tailbud into the PSM. Loss of Msgn1 reduces the flux of cells out of the tailbud, producing smaller somites and an enlarged tailbud, and, by delaying exhaustion of the progenitor population, results in supernumerary tail somites. Through its combined effects on gene expression and cell movement, Msgn1 (with Spt) plays a key role both in genesis of the paraxial mesoderm and in maintenance of the progenitor population from which it derives.

KEY WORDS: Mesogenin 1, Spadetail (Tbx16), Paraxial mesoderm

INTRODUCTION

The axial skeleton and skeletal muscles arise from the somites. As somites form from the anterior end of the presomitic mesoderm (PSM), mesoderm progenitors in the tailbud continually generate new mesoderm cells and feed them into the posterior PSM (Holley, 2007). The number of progenitors and the rate at which their progeny differentiate and move from the tailbud into the PSM must be controlled to ensure that the correct somite number is reached. Premature exhaustion of progenitors results in premature extinction of the PSM, a deficit of posterior somites, and therefore a truncated body.

Several mouse mutants with a truncated axis have been described and all but one result from lack of mesoderm (Wilson et al., 2009). The one exception carries a null mutation in the bHLH transcription factor mesogenin 1 (*Msgn1*). It lacks thoracic, lumbar and sacral vertebrae and skeletal muscles (Yoon and Wold, 2000), but there is no lack of mesoderm progenitors – quite the opposite: the lack of PSM tissue is accompanied by an enlarged tailbud containing an excess of cells expressing brachyury – a mesodermal progenitor marker. This suggests that in the absence of Msgn1, mesoderm progenitors that should normally emerge to become PSM remain instead in the tailbud. What, then, is the precise function of Msgn1? Do the brachyury-expressing progenitors remain in the tailbud because of a block in differentiation, cell migration, or both? To investigate this question, we characterised Msgn1 function through loss- and gain-of-function experiments combined with live imaging in zebrafish.

In zebrafish, *msgn1* is expressed in a domain similar to that in mouse (Yoo et al., 2003), but its function has not been described. However, the zebrafish *spadetail* (*spt*, now termed *tbx16*) mutant, like mouse *Msgn1* mutants, shows a large accumulation of cells expressing the brachyury-like gene *no tail* (*ntl*) in the tailbud (Griffin et al., 1998; Griffin and Kimelman, 2002). It has been proposed that Spt promotes the differentiation of tailbud progenitors by inhibiting the progenitor maintenance genes *ntl* and Wnt (Griffin and Kimelman, 2002; Martin and Kimelman, 2008). Spt also controls cell movement during gastrulation (Ho and Kane, 1990; Kimmel et al., 1989; Row et al., 2011), suggesting that Spt might also control motility in the tailbud. However, Spt cannot be the only factor regulating the transition of tailbud progenitors into PSM because *spt* null mutants still form tail somites (Griffen et al., 1998). Msgn1 is thus a candidate additional factor in zebrafish responsible for the switch from a tailbud progenitor state to a PSM state.

We show that combined loss of *msgn1* and *spt* leads to complete failure of trunk and tail somite formation accompanied by a large excess of *ntl*-expressing cells in the tailbud. Using a heat shock-inducible transgenic line, we find that a pulse of *msgn1* expression causes a rapid downregulation of *ntl* and *wnt8*, indicating that these two genes, which work in an intricate positive-feedback loop with each other, are themselves negatively regulated by Msgn1. This Msgn1-induced downregulation of *ntl* and *wnt8* expression is

[1]Instituto de Medicina Molecular e Instituto de Histologia e Biologia do Desenvolvimento, Faculdade de Medicina da Universidade de Lisboa, 1649-028 Lisboa, Portugal. [2]Instituto Gulbenkian de Ciência, P-2780-156 Oeiras, Portugal. [3]Department of Molecular and Cell Biology, University of California, Berkeley, CA 94720-3200, USA. [4]Division of Basic Science, Fred Hutchinson Cancer Research Center Seattle, WA 98109, USA. [5]Developmental Genetics Laboratory, Cancer Research UK London Research Institute, 44 Lincoln's Inn Fields, London WC2A 3PX, UK. [6]Vertebrate Development Laboratory, Cancer Research UK London Research Institute, 44 Lincoln's Inn Fields, London WC2A 3PX, UK.

*Authors for correspondence (ritafior@fm.ul.pt; msaude@fm.ul.pt)
‡Present address: Department of Molecular Genetics and Department of Molecular and Cellular Biochemistry, The Ohio State University, Columbus, OH 43210, USA

Accepted 13 September 2012

followed by ectopic activation of an intermediate/anterior PSM marker, *tbx24* (also known as *fss* and now termed *tbx6*), in the tailbud, consistent with the idea that Msgn1 throws a switch that converts cells from a tailbud progenitor state into a PSM state. *msgn1* expression is itself positively regulated by the *ntl*, Wnt and Fgf mesoderm progenitor maintenance genes (Griffin and Kimelman, 2002; Goering et al., 2003; Wittler et al., 2007; Wang et al., 2007; Morley et al., 2009; Garnett et al., 2009) (our data), which, by activating *msgn1* in a subset of the tailbud cell population, evidently trigger these cells to embark on the PSM differentiation pathway. We show that Msgn1 drives not only the differentiation but also the migration of such cells out of the tailbud into the PSM region. By governing the flux of cells from the progenitor region into the PSM, Msgn1 helps control both the size of somites and the size and persistence of the progenitor cell population; loss of Msgn1 activity thus gives rise to additional tail somites.

MATERIALS AND METHODS

Zebrafish lines and heat-shock experiments

Zebrafish lines: *msgn1*^{fh273} [a mutant found by screening ENU-mutagenised F1 fish (Draper et al., 2004)]; *spt*^{b104} (Kimmel et al., 1989); *ntl*^{b195} (Halpern et al., 1993); hsp70:*dkk1-GFP*^{w32} (Stoick-Cooper et al., 2007); and hsp70:*dnfgfr1-EGFP*^{pd1} (Lee et al., 2005).

For all heat-shock experiments, embryos were raised at 25°C and heat shocked at 39°C for the indicated time. hsp70:HA-*msgn1*, hsp70:*dkk1-GFP* and hsp70:*dnfgfr1-EGFP* embryos were generated from a cross between transgenic heterozygous and wild-type fish, giving batches with an expected mean ratio of 50% transgenics to 50% wild-type siblings. hsp70:HA-*msgn1* embryos were sorted into distinct phenotypic classes after in situ hybridisation (confirmed by genotyping) and hsp70:*dkk1-GFP* and hsp70:*dnfgfr1-EGFP* embryos were sorted by GFP expression.

DNA constructs

msgn1 cDNA was amplified from a zebrafish EST (IMAGE:7286125) with primers (5′-3′) pFWEcoRI (CCGGAATTCATGGCGCAAATCG-ACGTGGATG) and pRXbaI (CTAGTCTAGATCACTGCTGC-TCGAGGATGCC) and cloned into the *Eco*RI and *Xba*I sites of pCS2+, and *Not*I/SP6 was used to produce *msgn1* poly(A)-capped RNA and *Cla*I/T7 to produce an antisense RNA probe.

The hsp70:HA-*msgn1* transgenic was created by placing *msgn1* cDNA containing an N-terminal HA tag downstream of the *hsp70* heat-shock promoter in the pT2 vector (UAS-hsp70p-polyA-β-crystallin promoter-CFP) using primers pFW-HA-ClaI-Kozak (CCATCGATGGCCACC-ATGGCTTCATATCCTTACGATG) and pRStuI (AAAAGGCCTTTTTC-ACTGCTGCTCGAGGATGCC).

The nuclear localisation sequence (Nls)-tagged Kaede was generated by PCR. The first PCR was performed to add a *Bam*HI site and Kozak sequence to the 5′ end and part of the Nls and a linker sequence at the 3′ end of Kaede, using primers pFW1 (ATACGCGGATCCGCCGCCGCCATGAG-TCTGATTAAACCAGAAAATG) and pR1 (CTTTTCTTTTCTTTTTT-GGAGAACCCTTGACGTTGTCCGGCAATCC). The second PCR was performed to add an *Eco*RI site and the rest of the Nls sequence at 3′ end of Kaede, using primers: pFW1 and pR2 (TATCCGGAATTCTTAGTCAA-CTTTTCTTTTCTTTTTTGGAGA). The resulting PCR product was cloned into the *Bam*HI and *Eco*RI sites of pCS2+ and *Not*I/SP6 was used to produce *Nls-Kaede* poly(A)-capped RNA.

Microinjections

msgn1 morpholino (CATGGCGCAAATCGACGTGGATGTG) and a standard control morpholino (CCTCTTACCTCAGTTACAATTTATA) from Gene Tools were injected at 5.7 ng/embryo at the one-cell stage; 100 pg *msgn1*, *Nls-Kaede* and *Kaede* mRNAs were injected at the one-cell stage; the DNA plasmids *hsp70:ntl* and *hsp70:caβcatenin* (Martin and Kimelman, 2012) were injected at 30 pg/embryo at the one-cell stage.

In situ hybridisation and immunohistochemistry

Single whole-mount in situ hybridisations were performed as described (Thisse and Thisse, 2008). Double whole-mount fluorescent in situ hybridisations were performed as described (Jülich et al., 2005) with modifications: the red signal was developed with Fast Red (alkaline phosphatase substrate, Roche) and the green signal with tyramide-FITC (horseradish peroxidase substrate, PerkinElmer TSA Plus Fluorescein System). For HA immunohistochemistry, embryos were fixed for 2 hours in 4% paraformaldehyde, incubated with a monoclonal rat anti-HA antibody (3F10, Roche) followed by anti-rat DyLight 488 secondary antibody (Rockland). F-actin and nuclei were detected with Alexa Fluor 488-Phalloidin (Molecular Probes) and DAPI, respectively.

Kaede time-lapse microscopy

Kaede- and *Nls-Kaede* mRNA-injected embryos were kept in the dark. Eight-somite stage embryos were mounted in 1.2% low-melting agarose in glass-bottom Petri dishes. Small groups of cells were labelled by photoconversion in the maturation zone (25 μm posterior to the end of the notochord and in the focal plane of notochord and adaxial cells) and in the PSM (see Fig. 6H), with a 405 nm laser in a Zeiss 510 META confocal microscope using a 20× objective. Embryos were imaged in an Andor RevolutionXD spinning disc confocal microscope at 25°C. Stacks of 50 optical sections, spaced by 1 μm, were collected every 180 or 213 seconds for up to 2 hours.

Cell track analysis and measurements

Time-lapse movies were analysed using ImageJ software (NIH). Individual cells were tracked using the MtrackJ plug-in. The diving velocity and the anteroposterior (A/P) velocity were measured by following cells over an extended period of time (generally 60 minutes or more), and were calculated as $(z_{final}–z_{initial})/(t_{final}–t_{initial})$ and $(y_{final}–y_{initial})/(t_{final}–t_{initial})$, where z and y denote positions along the superficial/deep (dorsoventral) and A/P axes, respectively. The centre-to-centre distance between dot-2 and dot-3 was 109±5 μm (mean ± s.d.) – the same within narrow limits for all sets of embryos analysed. The mean A/P velocity of dot-3 cells was subtracted from the A/P velocity of dot-2 cells to obtain the A/P velocity (V_{ap}) of dot-2 relative to dot-3 cells. Statistical significance of differences between genotypes was calculated using unpaired two-tailed Student's *t*-test.

RESULTS

Depletion of *msgn1* and *spt* leads to complete loss of trunk and tail somites

To uncover the role of *msgn1* in zebrafish, we examined the embryonic phenotype in loss-of-function experiments using a translation-blocking morpholino (*msgn1MO*) (supplementary material Fig. S1A). *msgn1MO*-injected embryos showed increased *ntl* expression in the tailbud when compared with control siblings (Fig. 1A′,B′), as does the mouse *Msgn1* mutant (Yoon and Wold, 2000). However, somites formed in zebrafish *msgn1* morphants (Fig. 1B′,B″), in contrast to the mouse mutant, in which somite formation is abolished. To validate the *msgn1* knockdown, we analysed a zebrafish *msgn1* nonsense mutant allele, *msgn1*^{fh273} (supplementary material Fig. S1B). Homozygous *msgn1*^{fh273} mutants are viable and have a phenotype indistinguishable from that of the *msgn1* morphants (compare Fig. 1B-B″ with 1F-F″). The mildness of the *msgn1*^{fh273} phenotype is not due to a maternal contribution, as no maternal *msgn1* mRNA was detected either by in situ hybridisation or by RT-PCR and maternal-zygotic and zygotic *msgn1*^{fh273} mutants had indistinguishable embryonic phenotypes (data not shown). Another possible explanation for the mildness of the phenotype is a second Msgn gene, which is not unlikely given the genome duplication event in teleosts. However, we could not find any evidence for such a gene duplication.

The enlarged population of *ntl*-expressing tailbud cells in *msgn1* morphants and mutants is similar to that seen in *spt* mutants,

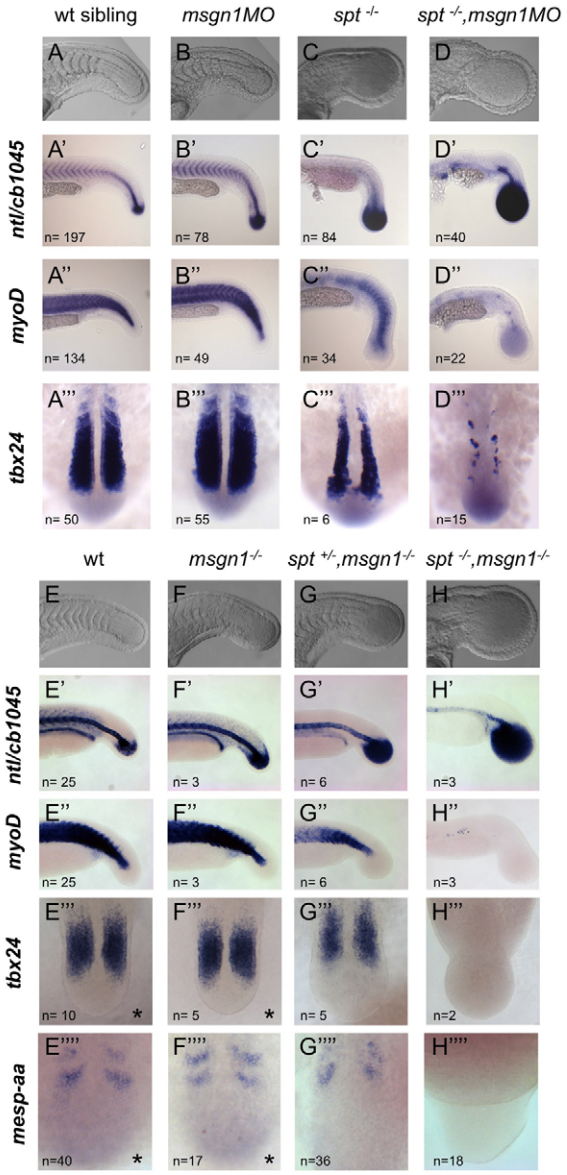

Fig. 1. Msgn1 and Spt are essential for tail somite formation. (**A-D**,**E-H**) Live zebrafish embryos typical of their genotypic classes. (**A′-D‴**,**E′-H‴**) In situ hybridisation for *ntl* and cb1045 (*xirp2a*), *myoD* (*myod1*), *tbx24* and *mespaa* expression in uninjected wild-type (wt) siblings and in the genotypes indicated. *spt*$^{-/-}$ mutants were derived from a heterozygous *spt*$^{+/-}$ cross. *msgn1*$^{-/-}$ mutants, *spt*$^{+/-}$;*msgn1*$^{-/-}$ mutants and *spt*$^{-/-}$;*msgn1*$^{-/-}$ double mutants were derived from a double heterozygous *msgn1*$^{+/-}$;*spt*$^{+/-}$ cross. Indicated is the number of embryos (*n*) observed with the phenotype shown in each panel, and when embryos were derived from mutant crosses the obtained *n* corresponded to the expected frequencies for each genotype. Asterisk indicates that wt and *msgn1* mutants have an undistinguishable phenotype at the 14-somite stage.

although less severe (Fig. 1C′) (Griffin and Kimelman, 2002). To test the hypothesis that Msgn1 and Spt function collaboratively, we injected *msgn1MO* into embryos derived from a cross of *spt* heterozygotes and we also generated *msgn1*$^{-/-}$;*spt*$^{-/-}$ double mutants. In both cases, the combined loss of Msgn1 and Spt led to a complete failure of trunk and tail somite formation along with a greatly enlarged tailbud that was full of *ntl*-expressing cells (Fig. 1D′,H′). This severe phenotype is very similar to that described for the *Msgn1* mouse mutant and strongly suggests that cells that should have emerged to form PSM remained instead in the tailbud progenitor region in an immature state. As further evidence of a shared function of *msgn1* and *spt*, loss of one copy of *spt* in an *msgn1* mutant or morphant background led to an enhanced *msgn1* phenotype (Fig. 1G-G‴; data not shown).

In wild-type embryos, the intermediate/anterior PSM is marked by expression of *tbx24* throughout somitogenesis; in *spt*$^{-/-}$ single mutants, *tbx24* expression is initially defective but is restored around the 14-somite stage, correlating with the recovery of somitogenesis at this stage in these mutants (Griffin and Kimelman, 2002) (Fig. 1C‴). By contrast, the combined absence of Msgn1 and Spt leads to a sustained loss of expression of *tbx24* (Fig. 1D‴,H‴) and *mespaa* (Fig. 1H‴), suggesting that embryos lacking Msgn1 and Spt function fail to generate somites because their cells are unable to progress along the PSM differentiation pathway.

Our data reveal a PSM formation program that differs between zebrafish and mouse. In the mouse, Msgn1 is required for both trunk and tail somite formation, but in zebrafish Spt is required for trunk somite formation and Msgn1 is not, whereas tail somite formation depends on both Msgn1 and Spt. To establish whether Msgn1 has a similar genetic relationship with Ntl during somitogenesis, we generated *msgn1*$^{-/-}$;*ntl*$^{-/-}$ double mutants; these did not display any enhancement of the *ntl* phenotype, suggesting that Msgn1 works downstream of Ntl and not in parallel to it (supplementary material Fig. S2).

Msgn1 regulates the transition from the tailbud maturation zone to the PSM

To determine the step of the PSM differentiation pathway at which Msgn1 acts, we analysed the *msgn1* morphant phenotype and compared this with the phenotype obtained when *msgn1* was overexpressed.

During normal development, mesoderm progenitors located in the dorsal tailbud region, which is known as the progenitor zone (PZ), express *ntl* and *wnt8* (Griffin and Kimelman, 2002) (Fig. 2A, dorsal view). The progeny of these cells that are destined to become PSM move ventrally to enter a so-called maturation zone (MZ), where they express *msgn1*, *spt* and *tbx6l*, in addition to *ntl* (Kanki and Ho, 1997; Griffin and Kimelman, 2002) (Fig. 2A ventral view, 2B-B″). When cells reach the posterior PSM, they downregulate *ntl* expression but maintain expression of *msgn1*, *spt* and *tbx6l* (Griffin and Kimelman, 2002; Amacher et al., 2002). A little later still, as cells become displaced from the posterior to the intermediate PSM, they start to express *tbx24* and will continue to do so until the somite border is completed (Nikaido et al., 2002) (Fig. 2A).

In *msgn1* morphants, the tailbud domain marked by *ntl* and *wnt8* was clearly expanded in comparison with control siblings (Fig. 2C-F′). Conversely, when *msgn1* was overexpressed by mRNA injection at the one-cell stage, expression of *ntl* and *wnt8* was severely reduced and lost prematurely (Fig. 2G-J′), followed later by a severely truncated tailbud (supplementary material Fig. S3I,J). Strikingly, *msgn1* overexpression led also to loss of the notochord as seen both by morphology and loss of midline *ntl* expression (Fig. 2H,H′; supplementary material Fig. S3L).

Double fluorescent in situ hybridisation for *ntl* and *tbx6l* showed that the tailbud PZ (identified by the expression of *ntl* but not *tbx6l*) and the MZ (located more deeply and identified by *ntl* and *tbx6l* co-expression) were both expanded in the absence of Msgn1 (Fig. 2K-L′). These data suggest that in the absence of Msgn1 there is a

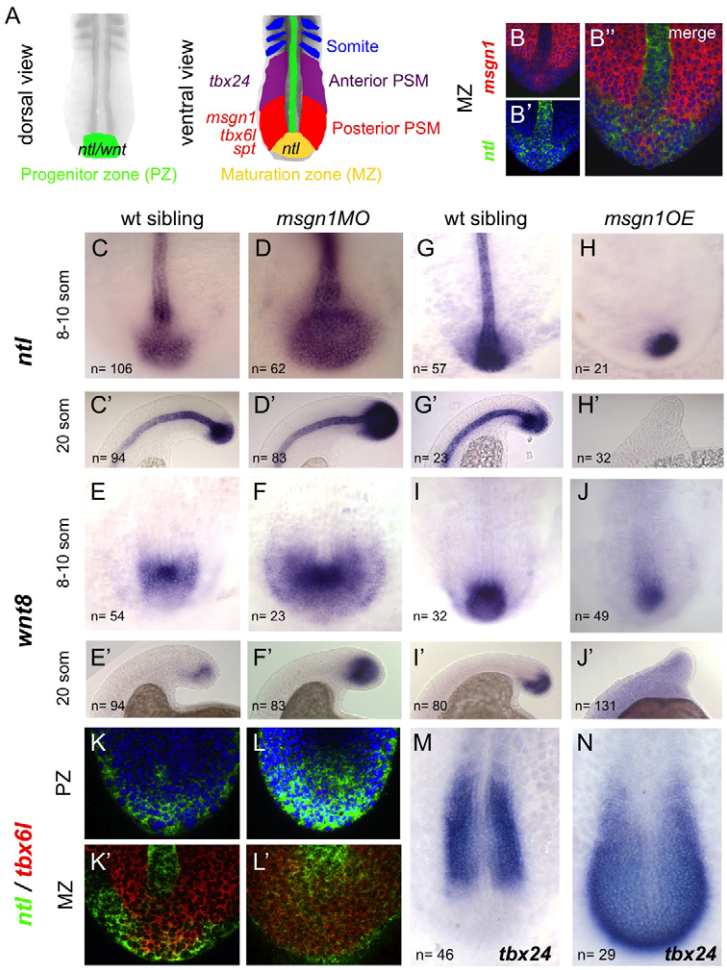

Fig. 2. Msgn1 regulates the transition from the maturation zone to the PSM. (**A**) Diagram of sequential gene expression as a mesodermal cell progresses from a progenitor state in the dorsal superficial tailbud until incorporation into a somite. (**B-B″**) Double fluorescent in situ hybridisation for *msgn1* (red) and *ntl* (green) in a wt zebrafish embryo. (**C-J′**) Expression of *ntl* (C-H′) and *wnt8* (E-J′) in *msgn1MO*-injected embryos (D,D′,F,F′) and their siblings (C,C′,E,E′) and in embryos overexpressing *msgn1* (H,H′,J,J′) and their siblings (G,G′,I,I′). At the 8- to 10-somite stage (H), 55% of *msgn1*-overexpressing embryos showed an absence of notochord *ntl* staining and 33% presented notochord breaks, but some expression of *ntl* was still evident in the tailbud. At the 20-somite stage (H′), 88% of these embryos showed an absence of *ntl* staining in the tailbud; this 88% consisted of 66% that showed no notochordal *ntl* expression and 22% that showed some notochord staining. In both H and H′, 12% of the injected embryos appeared wt. Seventy per cent of *msgn1OE* embryos showed continuing but strongly downregulated *wnt8* staining at the 8- to 10-somite stage (J); the remaining 30% exhibited a total absence of *wnt8* expression. By the 20-somite stage (J′), expression of *wnt8* had disappeared completely. (**K-L′**) Confocal images of double fluorescent in situ hybridisation showing expression of *ntl* (green) and *tbx6l* (red) in a *msgn1MO*-injected embryo (L,L′) and an uninjected sibling (K,K′) at the 8- to 10-somite stage, in the superficial dorsal progenitor region (K,L) and at the level of the notochord, where *ntl* and *tbx6l* expression overlap (K′,L′). (**M**,**N**) Expression of *tbx24* in a *msgn1* mRNA-injected embryo (N) and its sibling control (M) at the 8- to 10-somite stage.

reduction both in the flux of cells from the PZ state into the MZ state and in the flux from the MZ state into a PSM state: tailbud progenitors fail to progress normally through the PSM differentiation program. Consistent with this idea, when *msgn1* was overexpressed, the converse effect was seen: expression of *tbx24* was ectopically activated in the tailbud region (Fig. 2N), suggesting premature differentiation of mesoderm progenitors.

Msgn1 inhibits the Wnt/Ntl/Fgf loop and promotes progression along the PSM differentiation pathway

To clarify the dynamics of the regulatory interactions among *msgn1*, the tailbud progenitor marker genes *wnt3a*, *wnt8*, *ntl* and *fgf8*, and the PSM-specific genes *tbx24* and *tbx6l*, we created a zebrafish line containing a heat shock-inducible HA-tagged *msgn1* transgene (hsp70:HA-*msgn1*) that allowed us to activate *msgn1* in a time-controlled manner (supplementary material Fig. S4A-K′).

hsp70:HA-*msgn1* transgenics were heat shocked during segmentation, at a stage corresponding to the time when cells located in the tailbud are fated to contribute to trunk (supplementary material Fig. S4L-N′) or tail somites (Fig. 3). We observed a consistent and marked reduction of the levels of *ntl* and *wnt8*, and, to a lesser extent, of *wnt3a* and *fgf8*, in the tailbud of the hsp70:HA-*msgn1* transgenics as early as 1 hour post-heat shock (hpHS) (Fig. 3A-D′), suggesting that these genes are direct downstream targets of Msgn1. The effect was most rapid and striking for *ntl*, which was almost completely undetectable, whereas tailbud expression of *wnt3a*, *wnt8* and *fgf8* persisted at a reduced level for longer, but disappeared completely by 7 hpHS (Fig. 3H-J′).

Interestingly, in embryos fixed 7 hpHS, tailbud expression of *msgn1* itself was downregulated (supplementary material Fig. S4E′), suggesting that Msgn1 exerts a delayed negative feedback on its own expression. This is probably mediated through *ntl*, Wnt and/or Fgf genes: whereas Msgn1 has an inhibitory action on this set of genes, they themselves are known to be required for *msgn1* expression, not only during gastrulation (Griffin and Kimelman, 2002; Goering et al., 2003; Morley et al., 2009) but also during segmentation/tailbud stages (supplementary material Fig. S5C-F′). Moreover, this is consistent with the subtle but distinct expansion of *msgn1* mRNA expression in *msgn1* loss-of-function mutants (supplementary material Fig. S5A,A′).

Further insight into Msgn1 function comes from the timecourse of expression of *tbx24* after ectopic activation of Msgn1 expression, which is normally restricted to the intermediate/anterior PSM region (Fig. 3E,K,L). At 2 hpHS, *tbx24* expression was enhanced in its normal domain and was ectopically induced in the somites (Fig. 3E′). Strikingly, at 7 hpHS, we could detect *tbx24* expression also in the tailbud and midline of hsp70:HA-*msgn1* transgenics (Fig. 3K′); this expanded expression coincided with the time at which tailbud expression of *ntl*, *wnt8*, *wnt3a* and *fgf8* was completely abolished (Fig. 3G′-J′). The implication is that, in normal development, Msgn1 drives cells along the pathway of PSM differentiation, but that the progression to an

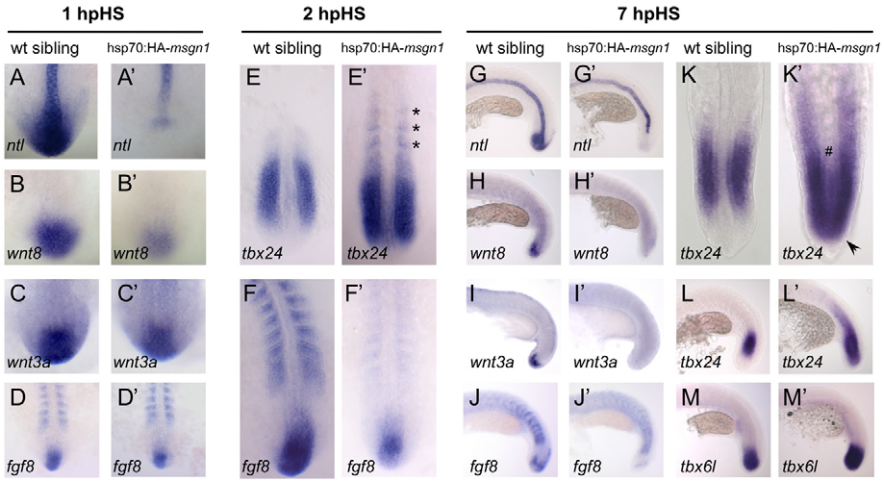

Fig. 3. A heat shock-driven pulse of Msgn1 inhibits expression of progenitor-specific genes and drives progression through the PSM differentiation program. Batches of zebrafish embryos comprising heat shocked hsp70:HA-*msgn1* transgenics along with wt sibling controls were analysed; ~50% of each batch showed a clear phenotype and were presumed to be the transgenics. (**A-D′**) Expression of *ntl*, *wnt8*, *wnt3a* and *fgf8* after 1 hour of recovery post-heat shock (hpHS) in hsp70:HA-*msgn1* embryos (A′-D′) and their wt siblings (A-D) heat shocked for 1 hour at the 13-somite stage. In the transgenics (32/59 embryos), tailbud expression of *ntl* was severely reduced (29/59 embryos) or totally eliminated (3/59 embryos). Tailbud expression of *wnt8* in the transgenics (35/65 embryos) was also strongly reduced, but reduction in expression levels of *wnt3a* and *fgf8* at this early time after heat shock was milder, making transgenics often hard to distinguish from sibling controls. (**E**,**E′**) *tbx24* expression at 2 hpHS. In the hsp70:HA-*msgn1* transgenics (29/76 embryos), *tbx24* expression is intensified in the PSM and abnormally extended into the region of formed somites, but is still absent from the tailbud. (**F**,**F′**) *fgf8* expression at 2 hpHS. In the hsp70:HA-*msgn1* transgenics (10/23 embryos), *fgf8* is downregulated but still detectable. (**G-M′**) Expression of *ntl*, *wnt8*, *wnt3a*, *fgf8*, *tbx24* and *tbx6l* at 7 hpHS. In the hsp70:HA-*msgn1* transgenics (G′, *n*=25/53; H′, *n*=46/92; I′, *n*=13/29; J′, *n*=32/66; K′, *n*=15/34; M′, *n*=10/22), the tailbud has now lost all expression of *ntl*, *wnt3*, *wnt8* and *fgf8* and instead expresses *tbx24* and *tbx6l*. Asterisks, arrowhead and hash sign indicate ectopic expression of *tbx24* in somites, tailbud and midline, respectively.

intermediate/anterior PSM state depends on escape from the influence of Ntl/Wnt/Fgf. This conclusion is further supported by our finding that, when Wnt signalling was transiently inhibited in hsp70:*dkk1* embryos, a posterior expansion of *tbx24* expression was indeed observed (Fig. 4).

Msgn1 controls the movements of mesoderm progenitor cells

As described above, our data showed that, in the absence of Msgn1, mesoderm progenitors accumulate in the tailbud, potentially reflecting a reduced flux of cells from this region into the PSM. This suggested that Msgn1 could be responsible for driving the cell movements that accompany differentiation along the PSM pathway. To test this, we used the Kaede photoconvertible fluorescent protein (Sato et al., 2006) to label small groups of cells in the tailbud region and to follow their movements, comparing normal control embryos with embryos with altered levels of Msgn1 (Fig. 5). We targeted our labelling on a plane at the level of the *msgn1*-expressing superficial layer of the MZ (at the same dorsoventral level as the notochord and adaxial cells).

In agreement with a previous report (Kanki and Ho, 1997), we observed that in *controlMO*-injected embryos, the marked cells dived from the superficial layer of the MZ into deeper layers (Fig. 5B-B″; supplementary material Movie 1) (i.e. along the *z*-axis of the confocal image stack) and then moved laterally into the PSM, avoiding the midline; once they reached the posterior PSM, they were displaced along the anteroposterior (A/P) axis as the embryo elongated (Fig. 5F-F″; supplementary material Movie 2).

In clear contrast to *controlMO*-injected embryos, ventral diving was markedly impaired in the absence of Msgn1 (Fig. 5C-C″; supplementary material Movie 3). Labelled cells located in the superficial layer of the MZ remained in the same *z*-focal plane for much longer in the absence of Msgn1 (compare Fig. 5D with 5H). We quantified this effect by tracking individual cells over a prolonged period (on average, 60 minutes) and calculated their mean diving velocity – that is, their net *z*-displacement divided by the period of observation. In *controlMO*-injected embryos, the mean diving velocity was 0.328 μm/minute (s.d.=0.21, *n*=39 cells/7 embryos). By contrast, in *msgnMO*-injected embryos, the mean diving velocity was only 0.001 μm/minute (s.d.=0.1, *n*=43 cells/7 embryos), significantly different from controls (*t*-test, $P<10^{-10}$). These results show that *msgn1* is required for the ventral diving of tailbud cells.

Msgn1-regulated cell movement may be mediated through negative regulation of *snail1a*

We next investigated how Msgn1 might control cell movements. The ventral diving of tailbud cells can be compared to the internalisation of germ ring cells during gastrulation, where an epithelial-to-mesenchymal (EMT)-like transition takes place (Marlow et al., 2004; Solnica-Krezel, 2006). We hypothesized that Msgn1 might regulate these EMT-like movements of tailbud cells during segmentation by regulating Snail expression or activity, as the Snail transcription factor family plays a role in EMT initiation in several contexts (Nieto, 2002). We investigated the expression of *snail1a* (also known as *snai1a*) – the only member of the zebrafish Snail family that is expressed in the tailbud (Blanco et al., 2007). During normal development, *snail1a* is strongly expressed in the MZ and fades in the PSM in a pattern that is largely complementary to, and non-overlapping with, that of *msgn1* (Fig. 6A-A″). We found that, in the

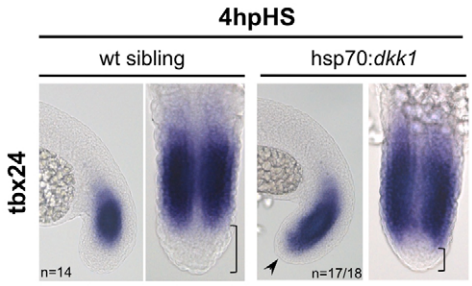

Fig. 4. Transient inhibition of Wnt signalling by Dkk1 allows ectopic activation of *tbx24* in the most posterior region of the PSM. Batches of zebrafish embryos comprising heat shocked hsp70:*dkk1* transgenics along with wt sibling controls were analysed. *tbx24* expression is shown at 4 hours of recovery after a 30-minute heat shock at the 13-somite stage, in lateral (left of each pair) and flatmount dorsal (right of each pair) views. Arrowhead indicates a posterior expansion into the tailbud of *tbx24* expression; bracket highlights the reduction of the tailbud region.

absence of *msgn1*, *snail1a* expression was upregulated and expanded anteriorly (Fig. 6D,E); a similar expansion has been reported in *spt* mutants (Thisse et al., 1993). Conversely, when *msgn1* was overexpressed by a short heat shock during segmentation, *snail1a* expression was severely and quickly downregulated 1 hpHS (Fig. 6G).

Since Msgn1 regulates *snail1a* expression during segmentation, we investigated the role of Snail1a in the control of tailbud cell movements. We followed Kaede photoconverted tailbud cells in embryos injected with *snail1aMO* (Blanco et al., 2007), comparing these with controls and with *msgn1MO*-injected embryos. In the absence of *snail1a*, the ventral diving movement from the superficial MZ (Fig. 6H, dot-1) was defective: the mean diving velocity was 0.05 μm/minute (s.d.=0.09, n=37 cells/4 embryos), significantly different from controls (t-test, $P<10^{-7}$) (Fig. 6I,J; supplementary material Movies 5, 6). The similarity between this result and the defective ventral diving observed in *msgn1MO*-injected embryos (supplementary material Movie 3), in which there is an excess of *snail1a* expression, suggests that a balanced level of Snail1a – not too much and not too little – is crucial for properly directed ventral diving movements in the MZ.

To further explore the role of *msgn1* and *snail1a* in A/P PSM extension, we marked and tracked Kaede photoconverted cells in the anterior and posterior PSM (Fig. 6H, dot-3 and dot-2). We converted our raw measurements of cell positions as a function of time into mean A/P velocities (V_{ap}) of the dot-2 cells relative to the dot-3 cells, reflecting the rate at which the intervening PSM tissue was extending or contracting along the A/P axis. Our data show that the A/P extension rate is significantly reduced in the absence of Msgn1 [Fig. 6K-L′, V_{ap} controls=0.15±0.05 μm/minute (dot-2 n=26 cells, dot-3 n=22 cells, 3 embryos); supplementary material Movies 7, 8 versus Fig. 6M-N′, V_{ap} *msgn1MO*=0.06±0.02 μm/minute (dot-2 n=22 cells, dot-3 n=22 cells, 3 embryos); t-test, P=0.007; supplementary material Movies 9, 10] and significantly increased in the absence of Snail1a [Fig. 6O-P′, V_{ap} *snail1aMO*=0.27±0.05 μm/minute (dot-2 n=31 cells, dot-3 n=37 cells, 4 embryos); t-test, $P<10^{-7}$; supplementary material Movies 11, 12]. Thus, Msgn1, possibly through Snail1a, controls cell movement not only at the point of origin of the paraxial mesoderm in the tailbud but also subsequently as the PSM cells mature. However, since the phenotype of loss of *snail1a* is very mild (supplementary material Fig. S6) (Blanco et al., 2007), it is likely that other factors are involved downstream of Msgn1.

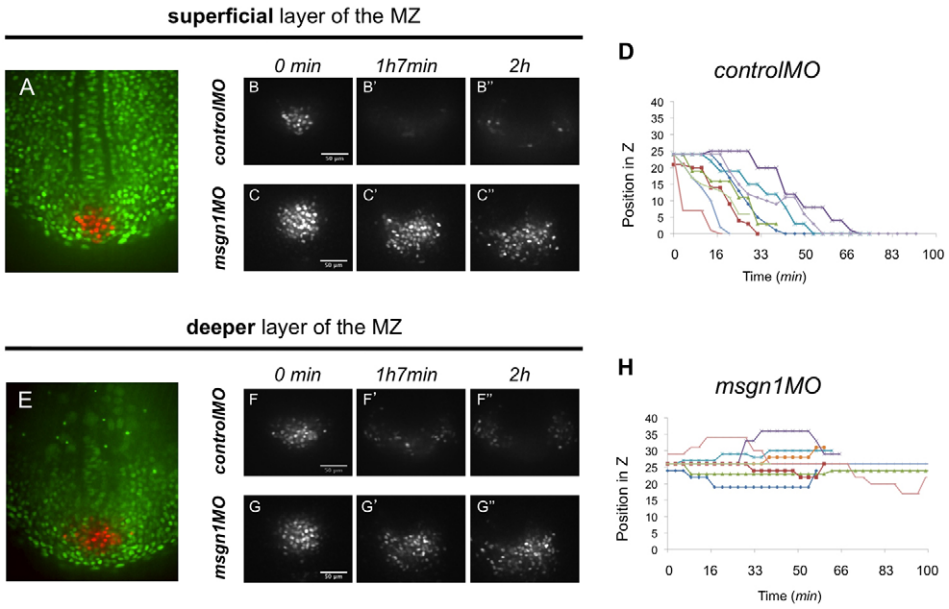

Fig. 5. Msgn1 controls cell movements in the neighbourhood of the tailbud. (**A**) An 8-somite stage Kaede-injected zebrafish embryo with a patch of tailbud cells freshly photoactivated (red), imaged in the plane of the notochord and adaxial cells [i.e. in the superficial layer of the maturation zone (MZ)]. (**B-C″**) Dispersion of the photoactivated tailbud cells imaged in this plane in *controlMO* (B-B″, Movie 1) and *msgn1MO* (C-C″, Movie 3) morphants. (**E**) An 8-somite stage embryo with photoactivated tailbud cells (red) imaged in a deeper layer, ~20 μm ventral to the notochord and adaxial cells (i.e. in a deep layer of the MZ). (**F-G″**) Dispersion of the photoactivated tailbud cells imaged in this plane in *controlMO* (F-F″, Movie 2) and *msgn1MO* (G-G″, Movie 4) morphants. (**D**,**H**) *z*-position of individual Kaede photoactivated tailbud cells tracked over time in *controlMO* (D) and *msgn1MO* (H) morphants. Each colour represents an individual cell. Loss of *msgn1* leads to failure of ventral diving and of the subsequent lateral dispersion. Scale bars: 50 μm.

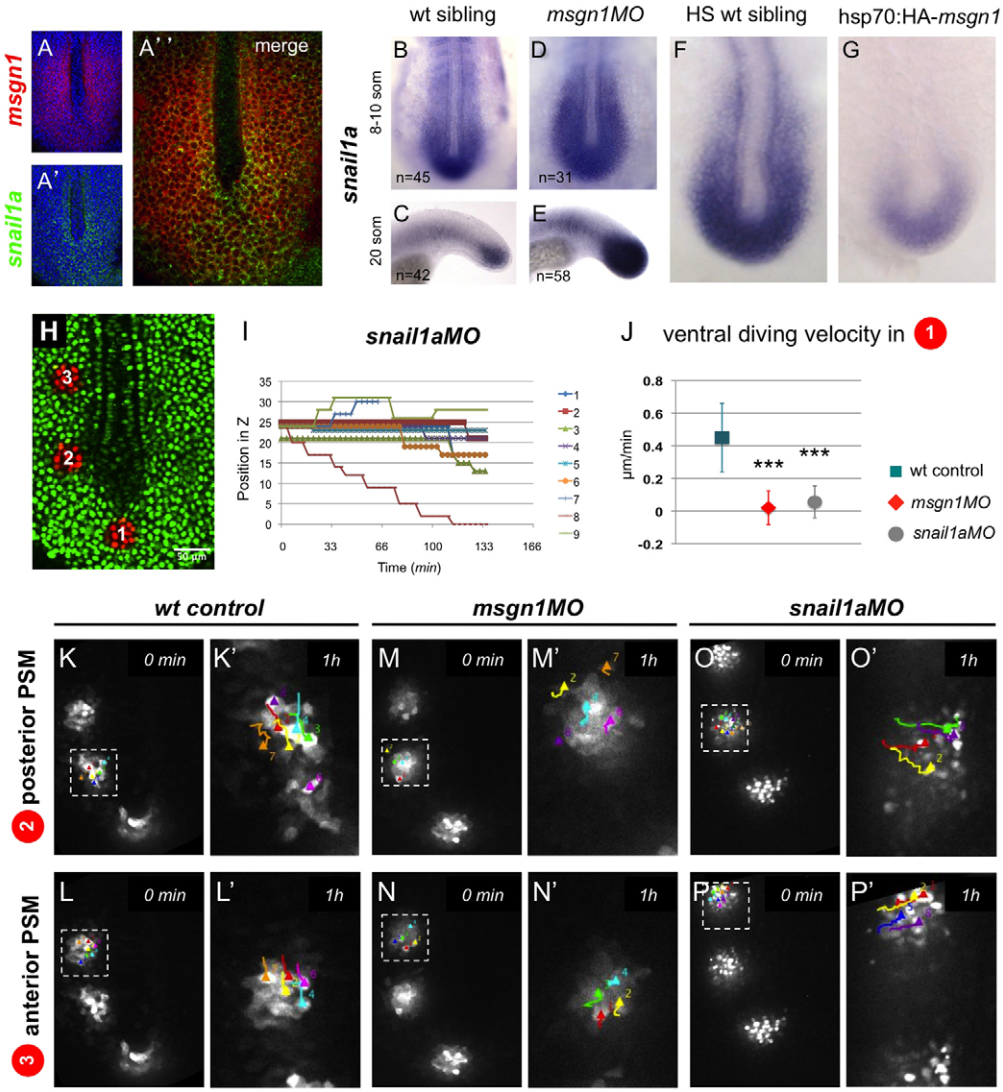

Fig. 6. Msgn1 regulates *snail1a* expression. (**A-A″**) Double fluorescent in situ hybridisation for *msgn1* (red) and *snail1a* (green) in a 10-somite stage wt zebrafish embryo, as seen in confocal section. (**B-E**) Expression of *snail1a* is increased in *msgn1MO* morphants (D,E) compared with sibling controls (B,C). (**F**,**G**) Expression of *snail1a* is decreased in hsp70:HA-*msgn1* embryos (G) compared with sibling controls (F) at 1 hpHS. (**H**) An 8-somite stage Kaede-injected embryo with freshly photoactivated cells (red) in the superficial layer of the MZ (region 1), in the posterior PSM (region 2), and in the anterior PSM (region 3). (**I**) *z*-position of individual cells photoactivated in region 1 in *snail1aMO* morphants, tracked over time. Each colour represents an individual cell. Compare with Fig. 5D,H. (**J**) Mean ventral diving velocities of cells marked by photoactivation in region 1, comparing wt control, *msgn1MO* and *snail1aMO* morphants. Mean ± s.d., ***P<0.0005 versus wt controls (*t*-test). (**K-P′**) Still images showing the tracks of posterior and anterior PSM photoactivated cells in wt control (K-L′), *msgn1MO*-injected (M-N′) and *snail1aMO*-injected (O-P′) embryos. The boxed regions in K-P are magnified in K′-P′. Scale bar: 50 μm.

Lack of Msgn1 leads to an increase in the number of tail somites accompanied by a reduction in their size

We have shown that, in *msgn1* mutants/morphants and in *msgn1* mutants lacking one copy of *spt*, somitogenesis is not blocked but that increased numbers of *ntl*/*wnt8*-positive progenitor cells are retained in the tailbud, suggesting that progenitor cells might persist there for an abnormally long time. If so, one might expect that somitogenesis would be prolonged, leading to an increase in the total number of somites produced. To test this, we counted the number of somites formed using the somitic boundary probe cb1045 (now termed *xirp2a*). Strikingly, in the absence of *msgn1* or in the *msgn1* enhanced phenotype (*msgn1*$^{-/-}$;*spt*$^{+/-}$), there was a significant increase in the number of somites formed (Fig. 7A,B,E-I). Whereas wild-type embryos produce on average 31.5 somites (s.d.=0.75, n=33), *msgn1*$^{-/-}$ mutants make 33 (s.d.=0.54, n=14; *t*-test, P=0.002) and *msgn1*$^{-/-}$;*spt*$^{+/-}$ mutants make on average 33.8 somites (s.d.=0.8, n=30; *t*-test, P=0.00001). *msgn1* morphants showed a very similar phenotype to *msgn1* mutants, with an increase in the average number of somites formed (mean=32.7, s.d.=1.18, n=23; *t*-test, P=0.006), whereas their wild-type siblings formed on average 31.6 somites (s.d.=0.72, n=23). The additional somites, in all these cases, were tiny and appeared as an extension of somitogenesis at the extreme tail end of the embryo (Fig. 7E-H), reflecting the abnormal persistence of a small population of progenitors there. We also saw effects on the pattern of somites more anteriorly, however: in the absence of *msgn1*, somites in the trunk and tail regions of the embryo were on average 15% smaller than in wild-type controls (*t*-test, P=0.002; Fig. 7C,D). This fits with the other indications that cells were being recruited into the PSM from the tailbud at a reduced rate during formation of the trunk and tail somites. To our knowledge, our findings in *msgn1* single and *msgn1*$^{-/-}$;*spt*$^{+/-}$ mutants represent the first experimental examples of genetic perturbations that leads to an increase in somite number.

DISCUSSION

As somites are being formed from the anterior region of the PSM, mesodermal progenitors have to constantly feed new cells into the posterior PSM. The numbers of progenitors and the rate at which they differentiate and move out from the tailbud to feed the PSM have to be tightly controlled, with termination of the process only when the correct species-specific number of somites is reached. With too fast a rate of exit, or too slow a proliferation of progenitors, the PSM would be prematurely extinguished and the body axis would be truncated. How is the balance between

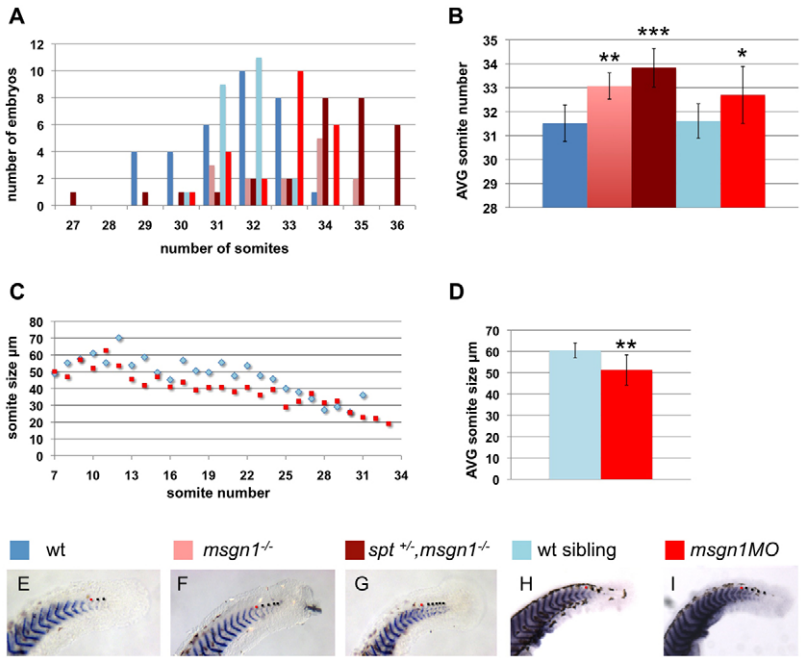

Fig. 7. Loss of Msgn1 affects somite number and size. Somite numbers and somite size in wt zebrafish embryos (blue and light blue), *msgn1*$^{-/-}$ single mutants, *spt*$^{+/-}$;*msgn1*$^{-/-}$ double mutants and *msgn1MO*-injected embryos (colours as indicated in E-I), fixed at 36 hours postfertilisation and measured after staining by in situ hybridisation with cb1045 to show somite boundaries. (**A**) Distribution of the total number of somites in the different genotypes. The peak of the distribution is at 32 somites for wt, 33 somites for *msgn1MO*, 33 somites for *msgn1*$^{-/-}$, and 34/35 somites for *spt*$^{+/-}$;*msgn1*$^{-/-}$. (**B**) The mean (±s.d.) number of somites for each genotype. **P*<0.01, ***P*<0.005, ****P*<0.0005, versus wt; *t*-test. (**C**) Size of somites as a function of position along the A/P body axis in *msgn1MO* morphants and wt siblings. (**D**) The mean (±s.d.) somite size in *msgn1MO* morphants and wt siblings. (**E-I**) Representative stained embryos of each genotype. The red dot in each case marks the thirtieth somite; black dots mark somites posterior to this.

differentiation and progenitor maintenance achieved and how is this coordinated with cell movement? In this work, we propose that Msgn1, acting in a semi-redundant fashion with Spt, plays a crucial role in controlling these processes (Fig. 8).

Msgn1 is required redundantly with Spt for tail formation in zebrafish

Loss of *msgn1* function in zebrafish causes a mild phenotype that is reminiscent of that observed in the mouse. In the absence of *msgn1*, the characteristic feature of retention of *ntl*/Wnt-positive progenitor cells in the tailbud is observed, although somites continue to be formed. However, when we generated *msgn1;spt* double mutants and morphants the tailbud was hugely enlarged and both trunk and tail somites fail to form (Fig. 1D-D″). These results reveal that *spt* and *msgn1* act redundantly in tail somite formation in zebrafish: either gene alone is sufficient to support the tail process. Although *msgn1* has been shown to be a Spt target during gastrulation (Garnett et al., 2009), our results show that *msgn1* cannot depend entirely on Spt for its activation but instead must act in parallel with Spt during tail formation.

Msgn1, like Spt, regulates the transition from the tailbud to the PSM by switching off the expression of progenitor genes

Previous work (Griffin and Kimelman, 2002) suggested that, for PSM progenitors to progress from the tailbud to the PSM, they must downregulate progenitor markers such as *ntl* and *wnt8*, and that Spt contributes to this regulation. To investigate whether Msgn1 is acting in a similar manner to Spt, we combined loss-of-function analysis with gain-of-function studies. We found that when *msgn1* is overexpressed ectopically, the *ntl*/*wnt8*-expressing progenitors are severely reduced and the anterior PSM marker *tbx24* is ectopically expressed in the tailbud (Fig. 2H,H′,J,J′,N). These results strongly suggest that Msgn1 is indeed acting like Spt (Griffin and Kimelman, 2002), inhibiting expression of the progenitor markers to allow cells to progress along the PSM differentiation pathway.

When we temporally controlled Msgn1 expression using our inducible *msgn1* transgenic, we observed rapid and strong downregulation of *ntl* and *wnt8* expression (Fig. 3A′,B′,C′), indicating that Msgn1 can rapidly inhibit the expression of these genes. Msgn1 does not have a readily identifiable repressor domain and is thought to be a transcriptional activator (Yabe and Takada, 2012), but it might exert repression via the rapid transcriptional activation of a repressor, or, for example, by dimerising with, and blocking the action of, some other bHLH family activator.

Use of the *msgn1* transgenic line also allowed us to show, for the first time, that the inhibition of progenitor character is essential for progression to the next step, i.e. the activation of the intermediate PSM marker *tbx24*. In fact, we show that Msgn1 can only ectopically activate *tbx24* in the tailbud (Fig. 3K′,L′) after a time delay that corresponds to the time required for the downregulation of *ntl*, Wnt and Fgf progenitor genes in the tailbud. This is further supported by the posterior expansion of *tbx24* upon transient inhibition of Wnt signalling during segmentation (Fig. 4).

msgn1 and the *ntl*, Wnt and Fgf genes are coupled in a negative-feedback loop

During segmentation, Ntl, Wnt and Fgf positively regulate *msgn1* expression (supplementary material Fig. S5) (Griffin and Kimelman, 2002; Goering et al., 2003; Wittler et al., 2007; Wang et al., 2007; Morley et al., 2009; Garnett et al., 2009), and we have shown that, in turn, Msgn1 represses *ntl*, Wnt and Fgf genes (Fig. 3), thereby establishing a negative-feedback loop.

How does this relate to the phenotypes that we see upon gain or loss of *msgn1* function? Our data show that, in the absence of *msgn1*, progenitors are retained longer in the PZ and MZ, as shown by *ntl* and *tbx6l* double in situ hybridisation. Normally, *msgn1* only starts to be expressed in the MZ and is not seen in the PZ, consistent with a role for Msgn1 in promoting the transition from the MZ to the PSM. But if Msgn1 is normally only expressed in the MZ and PSM, why does its loss cause an expansion of the PZ (Fig. 2L)? One possible explanation is based on the *msgn1*/*ntl*/Wnt/Fgf gene regulatory circuitry and the action of Wnt

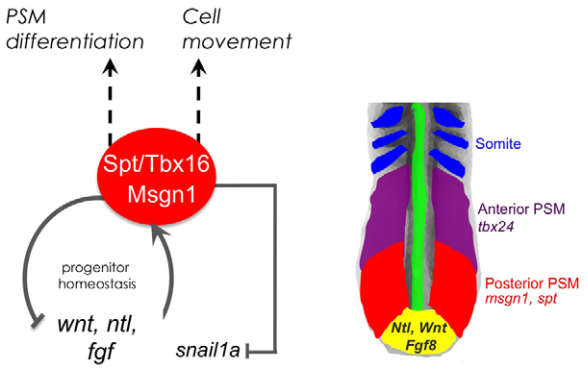

Fig. 8. Model of Msgn1 function. Progenitor cells in the tailbud are maintained by a positive-feedback loop between Wnt, *ntl* and Fgf genes. Wnt, Ntl and Fgf (or some combination of these factors) also activate the expression of *msgn1*, with a particular probability per progenitor cell per unit time (those that are fated to become PSM), driving cells out of the tailbud into the PSM. The presence of Msgn1 and Spt (Tbx16) in these emigrant cells stimulates their directed movement and also switches off expression of the Wnt/*ntl*/Fgf gene loop, allowing them to progress along the PSM differentiation pathway and activate *tbx24*. Msgn1 also represses *snail1a* to exert some or all of its effects on cell movement. The *msgn1/spt*-Wnt/*ntl*/Fgf negative-feedback loop might furthermore contribute to the homeostasis of the tailbud progenitor population: for example, an enlargement of the population of progenitor cells will tend to raise tailbud levels of Wnt and Fgf, which will increase the proportion of cells that switch on *msgn1/spt* and emigrate, bringing population size down again. PSM, presomitic mesoderm.

and/or Fgf as diffusible signals. Because Wnts can diffuse through the extracellular space, the increased expression of *wnt8* in the MZ, when Msgn1 is lost, could induce an upregulation of *ntl* and *wnt8* in the PZ, given that *ntl* and *wnt8* positively regulate one another (Martin and Kimelman, 2008).

We suggest that this complex negative-feedback relationship between *msgn1* and *ntl*/Wnt/Fgf governs the balance between the differentiation and maintenance of PSM progenitors.

Msgn1 regulates cell movement and axis elongation

Our time-lapse confocal microscopy analysis showed that in the absence of Msgn1 the ventral diving movement of tailbud cells is largely suppressed (Fig. 5H). To understand how Msgn1 controls cell movement during segmentation, we investigated whether Msgn1 could regulate Snail transcription factors, which are bona fide promoters of cell movement.

Indeed, we found that impaired Snail1a activity leads to deficient ventral diving (Fig. 6I). However, instead of activating *snail1a*, Msgn1 represses it (Fig. 6G). In fact, the endogenous expression pattern of *snail1a* seems to reflect this regulation, as *snail1a* is strongly expressed in the MZ and fades away in the PSM as *msgn1* starts to be strongly expressed (Fig. 6A-A″). These results suggest that Snail1a is important to initiate ventral diving movements, which are reminiscent of the EMT-like process that occurs at the germ ring, but as cells progress in the PSM it has to be turned off to allow cells to reduce their motility.

This is consistent with the recent finding that Spt is essential to stop the transitional highly motile state that cells adopt as they involute at the germ ring (Row et al., 2011). In *spt* mutants, *snail1a* is also upregulated in the tailbud (Thisse et al., 1993), and, as we have shown here, Spt and Msgn1 share partially redundant functions, suggesting that both Msgn1 and Spt might repress *snail1a* to complete the EMT-like movement in the tailbud.

Our results also show that Msgn1, through repression of *snail1a*, contributes to axis extension: in the absence of *msgn1* (expansion of *snail1a*) axis extension is reduced, whereas when *snail1a* is downregulated axis extension is increased. Why would stopping a motile state be important to promote axis elongation? A possible clue comes from recent work in the chick embryo that proposed that proper axis extension is dependent on a PSM cell motility gradient, i.e. effective A/P axis extension only occurs if the PSM cells reduce their motility as they become displaced anteriorly (Bénazéraf et al., 2010). Note that in zebrafish a similar gradient of cell motility has also been described in the PSM (Mara et al., 2007), reflecting the progressive epithelialisation of somite formation. In this scenario, following the ventral diving movement, efficient termination of Snail1a activity regulated by Msgn1/Spt could be required for the progressive reduction of PSM cell motility leading to efficient A/P axis extension in zebrafish.

Msgn1 regulates the number of somites by controlling the flux of cells out of the tailbud

According to the clock and wavefront model (reviewed by Dequéant and Pourquié, 2008), somite size should be proportional to the number of cells entering the PSM in each oscillation cycle of the segmentation clock, and the total number of somites should be equal to the total time for which production of PSM cells continues, divided by the length of that cycle. Our data fit these expectations, if we assume that the clock continues to tick at its normal rate in our mutants and morphants. Thus, for example, in the absence of Msgn1, where there is a reduced flux of cells from tailbud to PSM, somites are abnormally small (Fig. 7C,D). Moreover, retention of cells in the tailbud in *msgn1*$^{-/-}$ and *msgn1*$^{-/-}$;*spt*$^{+/-}$ mutants delays exhaustion of the stock of progenitors and allows somitogenesis to continue for longer than normal, leading to an increase in the final number of somites (Fig. 7A,B). To our knowledge, this is the first report of mutants that have an increased somite number. Although the effect that we see is small, our data suggest that modulation of the rate of exit of cells from the tailbud zone might be a strategy used during evolution to create the different species-specific somite numbers observed across vertebrates.

In summary, Msgn1, together with Spt, plays a central role in the production of paraxial mesoderm, controlling both a switch of cell character and cell movement, thereby propelling the transition from tailbud into PSM and driving the subsequent program of PSM differentiation.

Acknowledgements

We thank Stephen Wilson, David Kimelman and Randall Moon for *snail1a*, *ntl* and *wnt8* plasmids, respectively; Christian Tendeng for the pT2 vector; Ben Martin for the *hsp70:ntl* and *hsp70:caβcatenin* DNA constructs; the Yamaguchi, Feldman and Takada labs for sharing data prior to publication; Lara Carvalho, Fábio Valério, Jen St Hilaire, Deborah Weinman and Keely McDaniel for excellent fish care; José Rino and António Temudo for imaging advice; and Ana Margarida Cristovão and Pedro Henriques for technical support.

Funding

This work was supported by a Fundação para a Ciência e a Tecnologia (FCT) grant [PTDC/SAU-OBD/101282/2008 to L.S.]; an FCT Fellowship [SFRH/BPD/28586/2006 to R.F.]; Cancer Research UK (J.L.); a National Institutes of Health/National Institute of General Medical Sciences (NIH/NIGMS) grant [GM061952] and ARRA supplement (S.L.A.) and March of Dimes grant [1-FY09-458] (S.L.A.). A.A.M. is funded by an NIH Research Supplement

[NIH/NIGMS grant GM061952] to promote diversity in health-related research. The *msgnfh273* TILLING allele was found with support from NIH grant R01 HG002995. Deposited in PMC for release after 12 months.

Competing interests statement
The authors declare no competing financial interests.

Supplementary material
Supplementary material available online at
http://dev.biologists.org/lookup/suppl/doi:10.1242/dev.078923/-/DC1

References

Amacher, S. L., Draper, B. W., Summers, B. R. and Kimmel, C. B. (2002). The zebrafish T-box genes no tail and spadetail are required for development of trunk and tail mesoderm and medial floor plate. *Development* **129**, 3311-3323.
Bénazéraf, B., Francois, P., Baker, R. E., Denans, N., Little, C. D. and Pourquié, O. (2010). A random cell motility gradient downstream of FGF controls elongation of an amniote embryo. *Nature* **466**, 248-252.
Blanco, M. J., Barrallo-Gimeno, A., Acloque, H., Reyes, A. E., Tada, M., Allende, M. L., Mayor, R. and Nieto, M. A. (2007). Snail1a and Snail1b cooperate in the anterior migration of the axial mesendoderm in the zebrafish embryo. *Development* **134**, 4073-4081.
Dequéant, M. L. and Pourquié, O. (2008). Segmental patterning of the vertebrate embryonic axis. *Nat. Rev. Genet.* **9**, 370-382.
Draper, B. W., McCallum, C. M., Stout, J. L., Slade, A. J. and Moens, C. B. (2004). A high-throughput method for identifying N-ethyl-N-nitrosourea (ENU)-induced point mutations in zebrafish. *Methods Cell Biol.* **77**, 91-112.
Garnett, A. T., Han, T. M., Gilchrist, M. J., Smith, J. C., Eisen, M. B., Wardle, F. C. and Amacher, S. L. (2009). Identification of direct T-box target genes in the developing zebrafish mesoderm. *Development* **136**, 749-760.
Goering, L. M., Hoshijima, K., Hug, B., Bisgrove, B., Kispert, A. and Grunwald, D. J. (2003). An interacting network of T-box genes directs gene expression and fate in the zebrafish mesoderm. *Proc. Natl. Acad. Sci. USA* **100**, 9410-9415.
Griffin, K. J. and Kimelman, D. (2002). One-Eyed Pinhead and Spadetail are essential for heart and somite formation. *Nat. Cell Biol.* **4**, 821-825.
Griffin, K. J., Amacher, S. L., Kimmel, C. B. and Kimelman, D. (1998). Molecular identification of spadetail: regulation of zebrafish trunk and tail mesoderm formation by T-box genes. *Development* **125**, 3379-3388.
Halpern, M. E., Ho, R. K., Walker, C. and Kimmel, C. B. (1993). Induction of muscle pioneers and floor plate is distinguished by the zebrafish no tail mutation. *Cell* **75**, 99-111.
Ho, R. K. and Kane, D. A. (1990). Cell-autonomous action of zebrafish spt-1 mutation in specific mesodermal precursors. *Nature* **348**, 728-730.
Holley, S. A. (2007). The genetics and embryology of zebrafish metamerism. *Dev. Dyn.* **236**, 1422-1449.
Jülich, D., Geisler, R., Tübingen 2000 Screen Consortium and Holley, S. A. (2005). Integrinalpha5 and delta/notch signaling have complementary spatiotemporal requirements during zebrafish somitogenesis. *Dev. Cell* **8**, 575-586.
Kanki, J. P. and Ho, R. K. (1997). The development of the posterior body in zebrafish. *Development* **124**, 881-893.
Kimmel, C. B., Kane, D. A., Walker, C., Warga, R. M. and Rothman, M. B. (1989). A mutation that changes cell movement and cell fate in the zebrafish embryo. *Nature* **337**, 358-362.
Lee, Y., Grill, S., Sanchez, A., Murphy-Ryan, M. and Poss, K. D. (2005). Fgf signaling instructs position-dependent growth rate during zebrafish fin regeneration. *Development* **132**, 5173-5183.
Mara, A., Schroeder, J., Chalouni, C. and Holley, S. A. (2007). Priming, initiation and synchronization of the segmentation clock by deltaD and deltaC. *Nat. Cell Biol.* **9**, 523-530.
Marlow, F., Gonzalez, E. M., Yin, C., Rojo, C. and Solnica-Krezel, L. (2004). No tail co-operates with non-canonical Wnt signaling to regulate posterior body morphogenesis in zebrafish. *Development* **131**, 203-216.
Martin, B. L. and Kimelman, D. (2008). Regulation of canonical Wnt signaling by Brachyury is essential for posterior mesoderm formation. *Dev. Cell* **15**, 121-133.
Martin, B. L. and Kimelman, D. (2012). Canonical Wnt signaling dynamically controls multiple stem cell fate decisions during vertebrate body formation. *Dev. Cell* **22**, 223-232.
Morley, R. H., Lachani, K., Keefe, D., Gilchrist, M. J., Flicek, P., Smith, J. C. and Wardle, F. C. (2009). A gene regulatory network directed by zebrafish No tail accounts for its roles in mesoderm formation. *Proc. Natl. Acad. Sci. USA* **106**, 3829-3834.
Nieto, M. A. (2002). The snail superfamily of zinc-finger transcription factors. *Nat. Rev. Mol. Cell Biol.* **3**, 155-166.
Nikaido, M., Kawakami, A., Sawada, A., Furutani-Seiki, M., Takeda, H. and Araki, K. (2002). Tbx24, encoding a T-box protein, is mutated in the zebrafish somite-segmentation mutant fused somites. *Nat. Genet.* **31**, 195-199.
Row, R. H., Maître, J. L., Martin, B. L., Stockinger, P., Heisenberg, C. P. and Kimelman, D. (2011). Completion of the epithelial to mesenchymal transition in zebrafish mesoderm requires Spadetail. *Dev. Biol.* **354**, 102-110.
Sato, T., Takahoko, M. and Okamoto, H. (2006). HuC:Kaede, a useful tool to label neural morphologies in networks in vivo. *Genesis* **44**, 136-142.
Solnica-Krezel, L. (2006). Gastrulation in zebrafish – all just about adhesion? *Curr. Opin. Genet. Dev.* **16**, 433-441.
Stoick-Cooper, C. L., Weidinger, G., Riehle, K. J., Hubbert, C., Major, M. B., Fausto, N. and Moon, R. T. (2007). Distinct Wnt signaling pathways have opposing roles in appendage regeneration. *Development* **134**, 479-489.
Thisse, C. and Thisse, B. (2008). High-resolution in situ hybridization to whole-mount zebrafish embryos. *Nat. Protoc.* **3**, 59-69.
Thisse, C., Thisse, B., Schilling, T. F. and Postlethwait, J. H. (1993). Structure of the zebrafish snail1 gene and its expression in wild-type, spadetail and no tail mutant embryos. *Development* **119**, 1203-1215.
Wang, J., Li, S., Chen, Y. and Ding, X. (2007). Wnt/beta-catenin signaling controls Mespo expression to regulate segmentation during Xenopus somitogenesis. *Dev. Biol.* **304**, 836-847.
Wilson, V., Olivera-Martinez, I. and Storey, K. G. (2009). Stem cells, signals and vertebrate body axis extension. *Development* **136**, 1591-1604.
Wittler, L., Shin, E. H., Grote, P., Kispert, A., Beckers, A., Gossler, A., Werber, M. and Herrmann, B. G. (2007). Expression of Msgn1 in the presomitic mesoderm is controlled by synergism of WNT signalling and Tbx6. *EMBO Rep.* **8**, 784-789.
Yabe, T. and Takada, S. (2012). Mesogenin causes embryonic mesoderm progenitors to differentiate during development of zebrafish tail somites. *Dev. Biol.* **370**, 213-222.
Yoo, K. W., Kim, C. H., Park, H. C., Kim, S. H., Kim, H. S., Hong, S. K., Han, S., Rhee, M. and Huh, T. L. (2003). Characterization and expression of a presomitic mesoderm-specific mespo gene in zebrafish. *Dev. Genes Evol.* **213**, 203-206.
Yoon, J. K. and Wold, B. (2000). The bHLH regulator pMesogenin1 is required for maturation and segmentation of paraxial mesoderm. *Genes Dev.* **14**, 3204-3214.

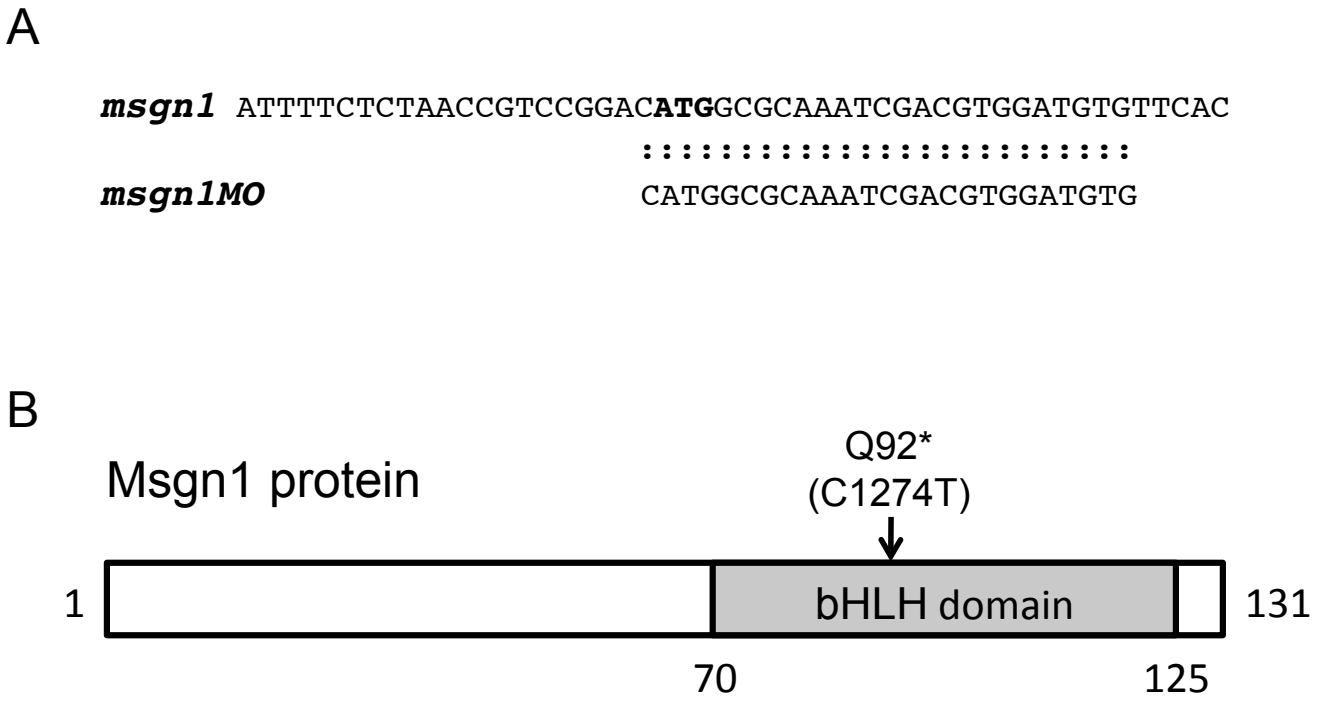

Fig. S1. Msgn1 loss-of-function strategies. (**A**) The *msgn1* morpholino oligonucleotide (*msgn1MO*) was targeted to the initiation ATG codon of the *msgn1* gene. (**B**) The *msgn^{fh273}* allele carries a point mutation that substitutes the cytosine at position 1274 with a thymine, changing the glutamine at position 92 into a stop codon. The resulting protein is truncated in the middle of the first helix of the HLH motif.

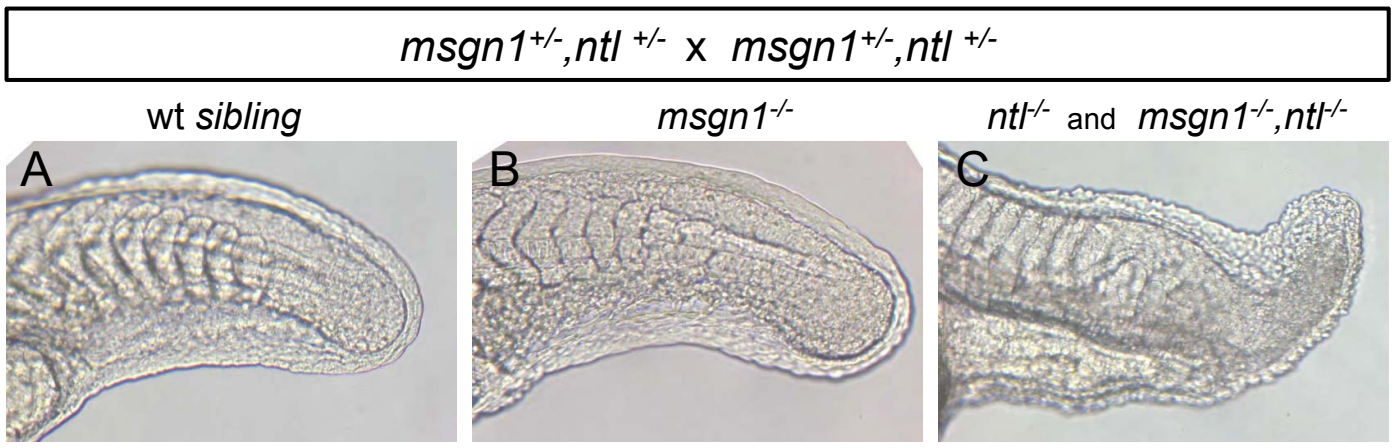

Fig. S2. Loss of *msgn1* does not enhance the tail deficiency of *ntl*$^{-/-}$ mutants. The progeny of a double heterozygous *msgn1*$^{+/-}$*;ntl*$^{+/-}$ cross were sorted into three distinguishable phenotypic classes and subsequent genotyping showed that embryos with a normal tail phenotype were wt (**A**), embryos with an enlarged tailbud were *msgn1*$^{-/-}$ (**B**) and embryos with similar severe tail truncations were either *ntl*$^{-/-}$ or *msgn1*$^{-/-}$*;ntl*$^{-/-}$ double mutants (**C**). Genotypes were present at the expected ratios.

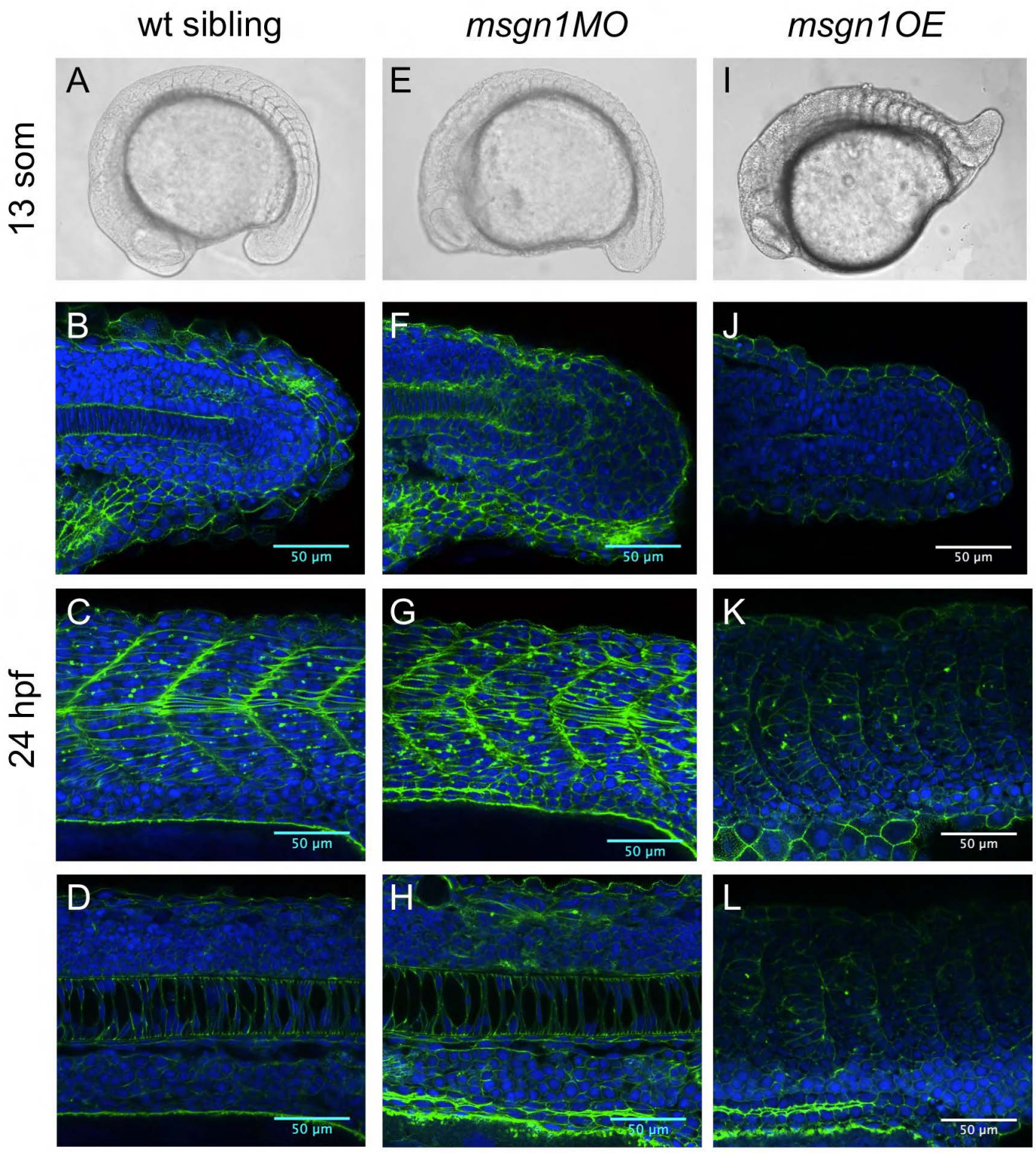

Fig. S3. Msgn1 regulates posterior development. (**A**,**E**,**I**) Live images of wt (A), *msgn1MO*-injected (E) and *msgn1*-overexpressing (I) embryos. (**B-D**,**F-H**,**J-L**) Nuclei (DAPI, blue) and F-actin (phalloidin, green) staining of wt (B-D), *msgn1MO*-injected (F-H) and *msgn1*-overexpressing (J-L) embryos. (B,F,J) Confocal sections at the level of the tailbud (B,F,J), the trunk somites (C,G,K) and the notochord (D,H,L).

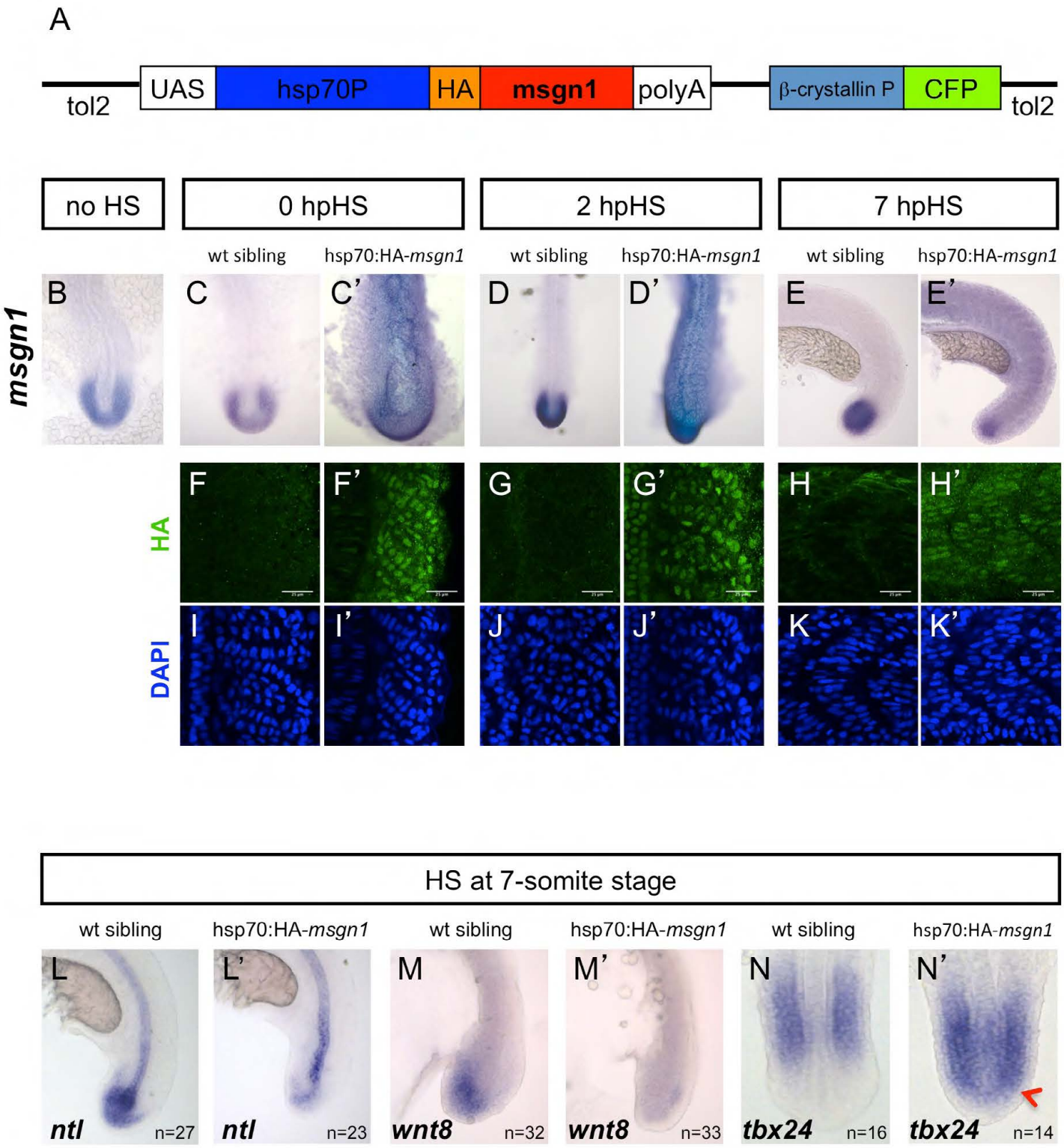

Fig. S4. Generation and validation of the hsp70:HA-*msgn1* transgenic line. (**A**) The construct used to generate the hsp70:HA-*msgn1* transgenic line. The N-terminus of the *msgn1* gene was fused with an HA tag and placed under an *hsp70* promoter. In addition, the β-*crystallin* promoter was used to drive CFP in the lens to facilitate identification of transgenic embryos. (B-N′) Embryos were obtained from a cross between hsp70:HA-*msgn1* heterozygous and wt fish, generating a batch with an expected frequency of 50% transgenics and 50% wt control siblings. (**B-E**′) In situ hybridisation showing *msgn1* mRNA levels in hsp70:HA-*msgn1* transgenic embryos and their wt sibling controls, with no heat shock (B) or heat shocked for 1 hour at the 13-somite stage and fixed immediately (C,C′), 2 hpHS (D,D′) and 7 hpHS (E,E′). (**F-K**′) Levels of HA-tagged Msgn1 protein (F-H′) at the level of the tenth somite in hsp70:HA-*msgn1* transgenic embryos fixed immediately after heat shock (0 hpHS), 2 hpHS and 7 hpHS and their corresponding control siblings. (I-K′) The same embryos as in F-H′ counterstained with DAPI to reveal the nuclei. (**L-N**′) Expression of *ntl*, *wnt8* and *tbx24* in hsp70:HA-*msgn1* transgenic embryos and their respective control siblings heat shocked for 1 hour at the 7-somite stage and fixed 7 hpHS. Red arrowhead, ectopic expression of *tbx24* in the tailbud. hpHS, hours post-heat shock.

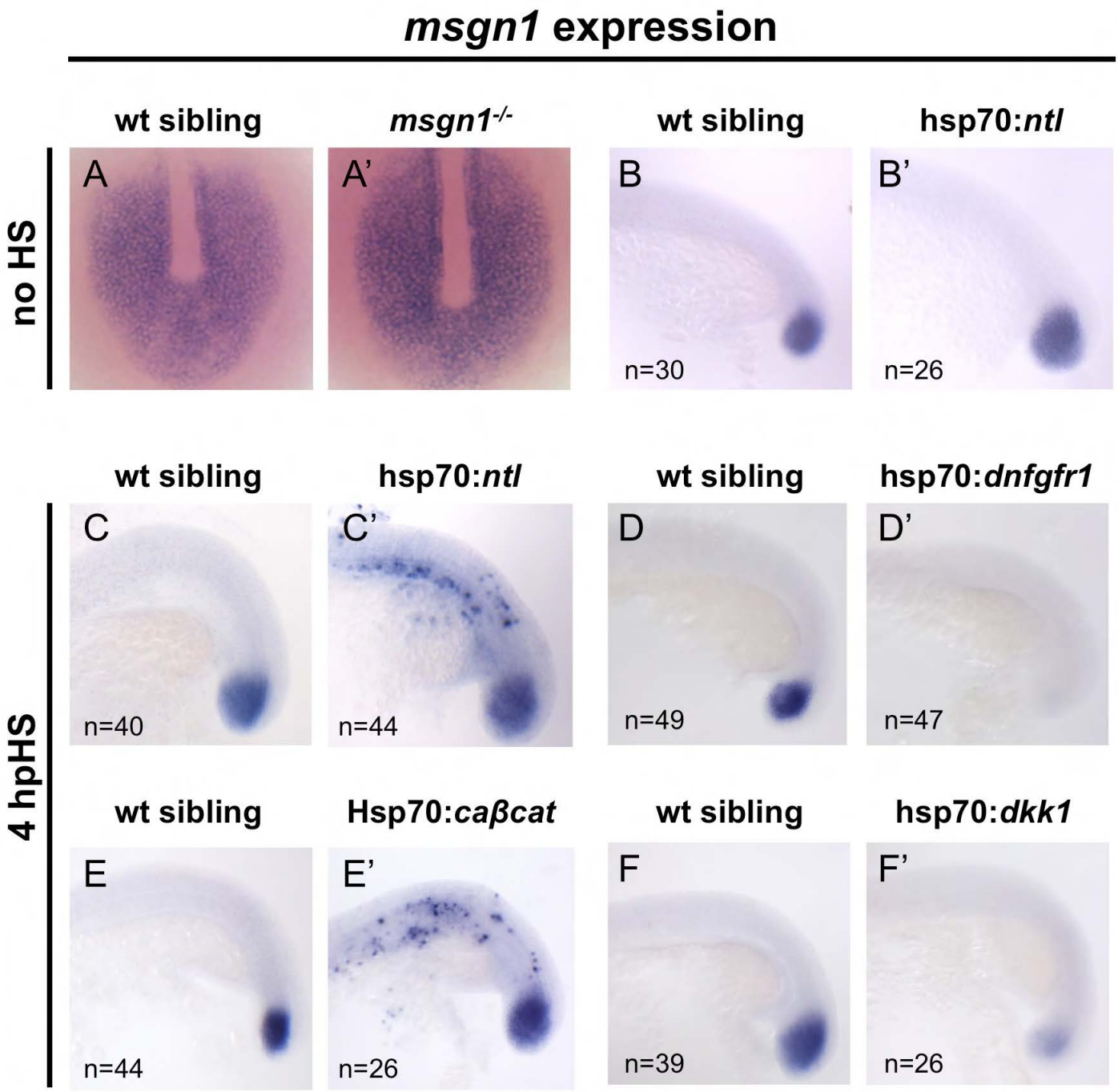

Fig. S5. Regulation of *msgn1* expression during segmentation. (**A**,**A′**) Similar expression of *msgn1* in the presomitic mesoderm of 8-somite stage embryos was detected in wt siblings (A) and *msgn1*$^{-/-}$ embryos (A′). (**B**,**B′**) With no heat shock, a normal pattern of expression of *msgn1* is observed in hsp70:*ntl* injected embryos and their uninjected siblings. (C-F′) All embryos were heat shocked for 30 minutes at the 13-somite stage. (**C**,**C′**) Ectopic expression of *msgn1* is induced in hsp70:*ntl* injected embryos when compared with their uninjected siblings. (**D**,**D′**) A complete absence of *msgn1* expression is observed in hsp70:*dnfgfr1* transgenic embryos when compared with their siblings. (**E**,**E′**) Ectopic expression of *msgn1* is induced in hsp70:*caβcat* injected embryos when compared with their uninjected siblings. (**F**,**F′**) A severe downregulation of *msgn1* expression is observed in hsp70:*dkk1* transgenic embryos when compared with their siblings. Transgenic embryos were obtained from a cross between heterozygous transgenics and wt fish, generating batches with the expected frequency of 50% transgenics and 50% wt control siblings.

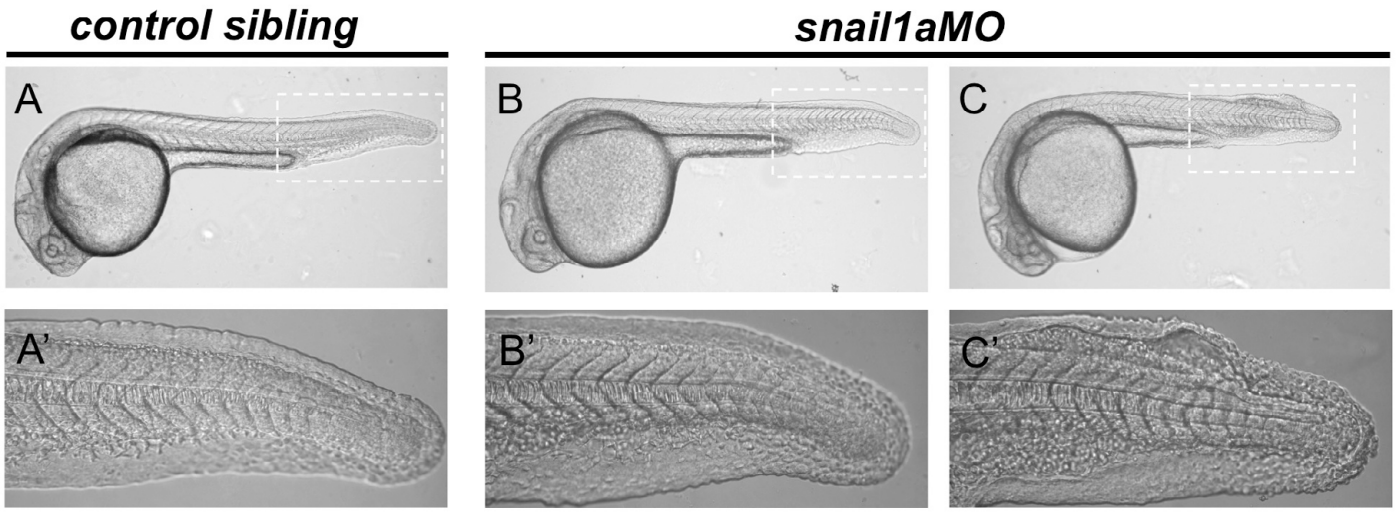

Fig. S6. The mild *snail1a* loss-of-function phenotype. Eighty percent (*n*=123, three different batches) of the *snail1aMO*-injected embryos (**B**,**B′**) show an indistinguishable phenotype from controls (**A**,**A′**) and 20% show a fin-fold phenotype (**C**,**C′**). (A′-C′) Magnification of the tail region corresponding to the embryos shown in A-C.